



# Design, Synthesis, Characterization and Application of BNPs@SiO<sub>2</sub>(CH<sub>2</sub>)<sub>3</sub>NH-CC-AMP-Pd (0) as a New Reusable Nano-Catalyst for Suzuki and Heck Cross-Coupling Reactions

Minoo Khodamorady<sup>1</sup> · Kiumars Bahrami<sup>1,2</sup>

Received: 5 September 2019 / Accepted: 24 November 2019  
© Springer Science+Business Media, LLC, part of Springer Nature 2019

## Abstract

A simple and effective method was used for the successful preparation of the Boehmite@(CH<sub>2</sub>)<sub>3</sub>NH-CC-AMP-Pd (0) NPs as an environmentally friendly heterogeneous nano-catalyst. The synthesized nano-catalyst was well identified by different techniques like FT-IR, XRD, XPS, TEM, SEM, EDX, TGA, mapping, and ICP analysis. The BNPs@SiO<sub>2</sub>(CH<sub>2</sub>)<sub>3</sub>NH-CC-AMP-Pd was used as a recoverable nano-catalyst for Suzuki-Miyaura and Mizoroki-Heck coupling reactions under mild, green and sustainable conditions with excellent yields (H<sub>2</sub>O, EtOH as solvent for Suzuki reaction and solvent-free conditions for Heck reaction). Also, the distribution of palladium on the catalyst surface is uniform and the average palladium size is between 20 and 30 nm. Compared to similar works, this protocol has some of the important aspects such as: thermal and mechanical stability of the catalyst, low palladium leaching (9.7%), the simplicity of the preparation, the availability of raw materials, not expensive, no need for neutral atmosphere, appropriate times, green conditions, use low amount of catalyst (1.42 mol%) and reused catalyst for several consecutive times (at least seven times).

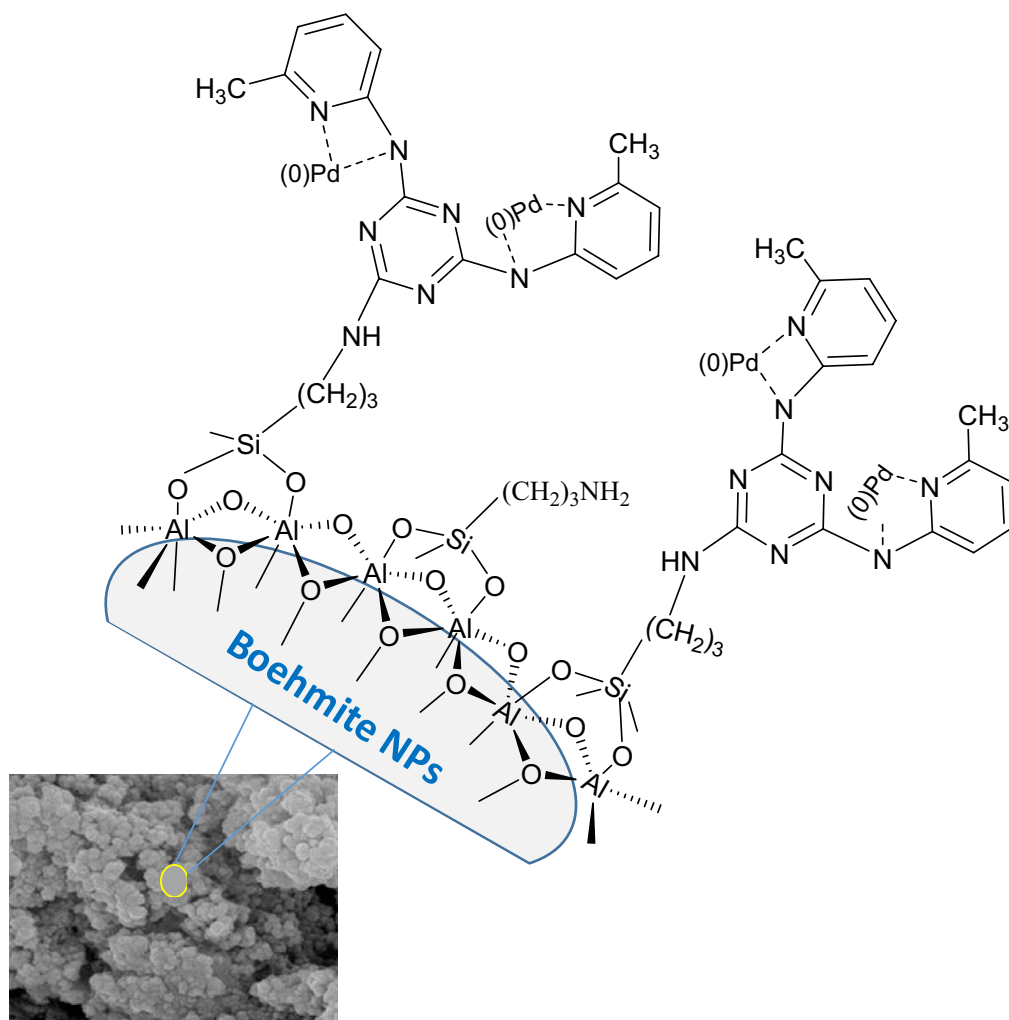
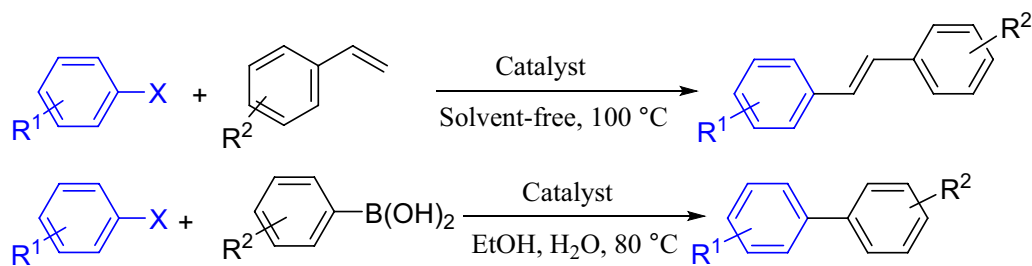
---

✉ Kiumars Bahrami  
kbahrami2@hotmail.com; k.bahrami@razi.ac.ir

<sup>1</sup> Department of Organic Chemistry, Faculty of Chemistry, Razi University, Kermanshah 67149-67346, Iran

<sup>2</sup> Nanoscience and Nanotechnology Research Center (NNRC), Razi University, Kermanshah 67149-67346, Iran

## Graphic Abstract



Catalyst = BNPs@SiO<sub>2</sub>(CH<sub>2</sub>)<sub>3</sub>NH-CC-AMP-Pd (0)

**Keywords** Boehmite · Suzuki and heck reactions · Cyanuric chloride · 2-Amino-6-methyl pyridine · Pd-catalyzed

## 1 Introduction

Today significant developments in nanotechnology have led to an increase in the performance of nano-catalysts [1].

Nano-catalysts are divided into heterogeneous and homogeneous catalysts. According to our knowledge, homogeneous catalysts are more active than heterogeneous catalysts due to easy contact between active sites on the catalyst and

the reactants in the solution, but it is difficult to isolate and recover these catalysts [2]. Nowadays, nanotechnology makes it possible to design and construct heterogeneous nanoscale catalysts, which, on the one hand, have advantages, such as high surface area and better particle size and shape, and on the other hand, these catalysts have activity and selectivity as well as homogeneous systems, and due to insolubility in water and most organic solvents, they can easily be separated and recycled. Therefore, the use of renewable heterogeneous nano-catalysts for the development of green chemistry and engineering is inevitable [3]. In addition, considering the prevalence of chemistry in the industry and the chemical production and synthesis of organic materials, the design of catalysts and environmentally friendly high-surface-area solid is essential.

According to the aforementioned, today, the design and selection of appropriate ligands in coordination chemistry is very significant, because one of the factors that can reduce particle size and increase the surface area of the nano-catalyst is the type of ligand.

The proper ligand not only prevents the aggregation and deposition of particles but also influences the orderly and uniform placement of the particles on the surface of the nano-catalyst.

In recent years, the use of various ligands on the surface of the catalysts and composites has been considered due to their stabilizing properties. Indeed, different organic and mineral supports have been used such as charcoal, inorganic silica, alumina, carbon nanotube, synthetic polystyrene [4–7] and magnetic nanoparticles (MNPs) supports [8].

In the following, we introduce boehmite as a suitable and sustainable support. Boehmite is an aluminum oxide hydroxide and has an orthorhombic structure and many hydroxyl groups are located on its surface [9]. Boehmite comes from inexpensive and non-toxic raw materials in the presence of water as solvent at room temperature in appropriate conditions (without the need for inert atmosphere and calcination) and has unique properties such as lack of sensitivity to weather, thermal and mechanical stability, high dispersity of the active phases, non-toxicity and ease of surface modification [10–13]. More important, boehmite nanoparticles (BNPs) are excellent support for heterogenization of catalysts due to the high chemical stability, availability, biocompatibility, low cost and corrosion resistance [13–15].

Boehmite is also used as cosmetic products, coating, adsorbent, catalyst, vaccine adjuvants, optical material, and composite reinforcement material in ceramics [16–18].

Many methods have been proposed for the synthesis of boehmite based on its chemical and physical properties [17], but modification of boehmite as heterogeneous support is rarely reported [19]. It should be noted that various factors affect the synthesis of metallic nanoparticles with suitable

catalytic properties such as particle size, crystalline structure and the nature of ligand [20–22].

Over the past decades, various catalytic systems including intermediate metals such as copper [22, 23], iron [24], nickel [25], cobalt [26, 27], and palladium [28, 29] have been taken into consideration.

Today, the formation of carbon–carbon bonds as one of the major reactions in organic chemistry has attracted a great deal of attention because cross-reactions are powerful tools in both academic and industrial laboratories and the most commonly used methods for carbon–carbon bonding are Suzuki and Heck reactions. The cross-coupling reactions are considered as key steps in production of complex biological molecules and pharmaceutical like cozaar<sup>®</sup> [30], (+)-dynamycin [31], morphine [32], and paclitaxel (Taxol<sup>®</sup>) [33]. Additionally, coupling reactions catalyzed with palladium nanoparticles are one of the most important and powerful methods for carbon–carbon bonding [34–37]. Two of the old methods for the formation of carbon–carbon bonding are the use of palladium salts [38–40] and palladium homogenous catalysts [41, 42]. Of course, these methods still have environmental restrictions and cannot be recycled or reused. Given the cases mentioned and the fact that palladium is expensive, toxic and rare, the researchers have focused on the heterogeneity of palladium catalysts, which is very important from both environmental and economic points of view [43–45].

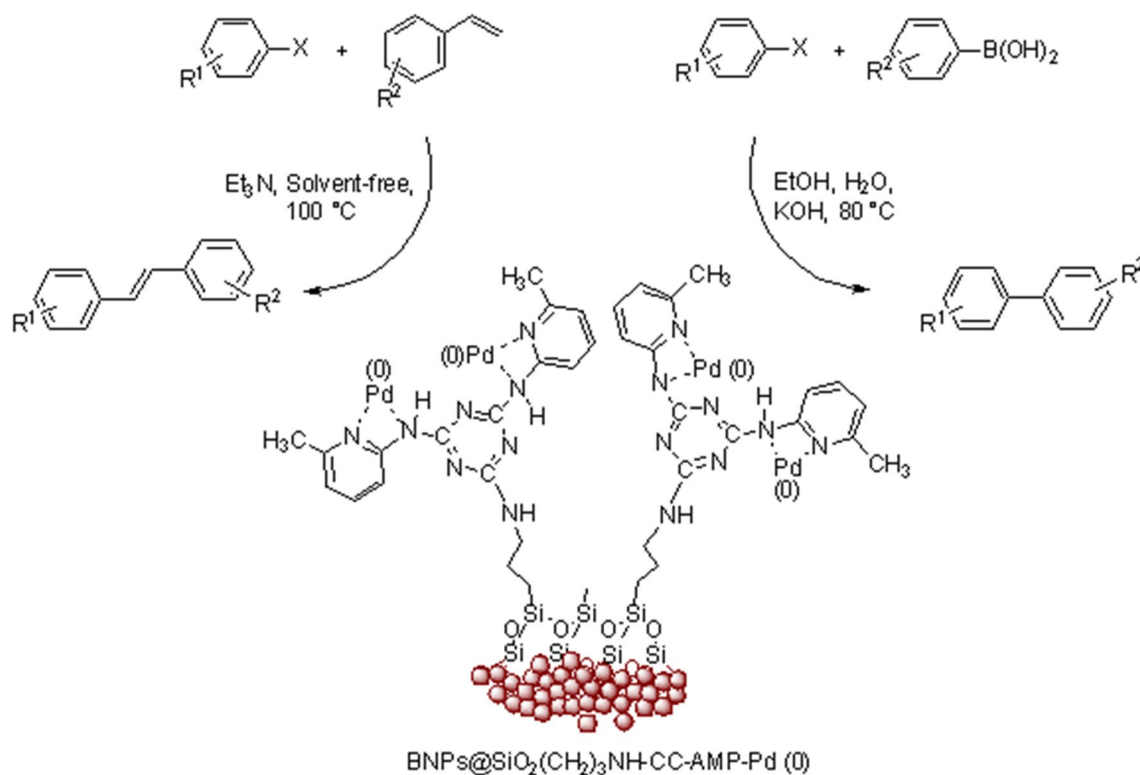
Inspired by recent progresses in the field of nano-catalyst, in this contribution, we reported the synthesis of boehmite-supported palladium cyanuric chloride-2-amino-6-methylpyridine complex (BNPs@SiO<sub>2</sub>(CH<sub>2</sub>)<sub>3</sub>NH-CC-AMP-Pd(0)) through a simple process without the need for strict conditions.

This nano-catalyst found to be stable, efficient, cheap and reusable catalyst for the formation of C–C bonds such as Suzuki reactions using phenylboronic acid with aryl halides in H<sub>2</sub>O:EtOH (1:1) at 80 °C and Heck reactions using styrene with aryl halides in solvent-free conditions at 100 °C (Scheme 1).

## 2 Experimental

### 2.1 General

The materials were purchased from Merck and Fluka. All reactions were monitored by TLC. Stuart Scientific SMP2 apparatus was used for the determination of Melting points. FT-IR spectra were determined with a PerkinElmer 683 instrument. Thermogravimetric analysis (TGA) was carried out with a STA PT-1000 Linseis instrument (Germany) under air atmosphere at a heating rate of 10 °C min<sup>-1</sup>. FESEM and energy-dispersive X-ray (EDX) measurements



**Scheme 1** Synthesis of biphenyl and trans-stilbene derivatives with BNP@SiO<sub>2</sub>(CH<sub>2</sub>)<sub>3</sub>NH-CC-AMP-Pd (0)

were performed using a TESCAN- MIRA3 operated at 26 kV with the electron gun filament: tungsten. TEM images were carried out with a Zeiss-EM10C (Germany) operating at 100 kV. The elemental palladium content of nano-catalyst was determined by Perkin Elmer Optima 7300D inductively coupled plasma (ICP). X-ray powder diffraction (XRD) was performed on a PANalytical Company X'Pert Pro MPD diffractometer with Cu K $\alpha$  radiation ( $\lambda = 0.154$  nm). The chemical composition of the catalyst on the surface of the boehmite was performed using X-ray Photoelectron Spectroscopy (XPS), a Kratos Axis Ultra-DLS spectrometer with an Al K $\alpha$  as a source. The data was recorded by CasaXPS software.

## 2.2 Preparation of the Catalyst

A solution of NaOH (6.490 g) in 50 mL of distilled water was added dropwise to a solution of Al(NO<sub>3</sub>)<sub>3</sub>·9H<sub>2</sub>O (20 g) in 30 mL of distilled water under vigorous stirring. The resulting milky mixture was subjected to mixing in an ultrasonic bath for 3 h at 25 °C. The resulting nano-boehmite was filtered and washed with distilled water and kept in an oven at 220 °C for 4 h. Then the obtained boehmite nanoparticles (1.5 g) were dispersed in 50 mL ethanol and 10 mL of deionized water and for the hydrolysis and condensation, TEOS was used as

silica source (2 mL) and then PEG (5.36 g), ammonia solution (10 mL) were respectively added to the mixture and continuously reacted at room temperature for 38 h. Then, the product (boehmite-silica) was filtered and washed with ethanol and distilled water, the obtained boehmite-silica was dried at room temperature. Then, APTMS (2 mL) was added to boehmite-silica and the mixture was dispersed in toluene (12 mL) and the resulting BNP@SiO<sub>2</sub>(CH<sub>2</sub>)<sub>3</sub>NH<sub>2</sub> was filtered, washed with ethanol and dried at 70 °C. In the next step, cyanuric chloride (2 g) was added to the BNP@SiO<sub>2</sub>(CH<sub>2</sub>)<sub>3</sub>NH<sub>2</sub> (1 g). The mixture was sonicated for 30 min and stirred under reflux in toluene for 24 h. In the following, a mixture of the BNP@SiO<sub>2</sub>(CH<sub>2</sub>)<sub>3</sub>NH<sub>2</sub>-CC (0.90 g) and 2-amino-6-methyl-pyridine (AMP) (1 g) were exposed to reflux in toluene for 24 h. after that, the resulted BNP@SiO<sub>2</sub>(CH<sub>2</sub>)<sub>3</sub>NH<sub>2</sub>-CC-AMP was filtered, washed with ethanol and dried at 70 °C. In the final step, BNP@SiO<sub>2</sub>(CH<sub>2</sub>)<sub>3</sub>-CC-AMP (0.8 g) was dispersed in 25 mL ethanol and then palladium chloride 0.12 g was added to the reaction mixture and reaction stirred at 70 °C for 8 h. The final product BNP@SiO<sub>2</sub>(CH<sub>2</sub>)<sub>3</sub>NH-CC-AMP-Pd (0) was filtered, washed with ethanol and dried at 60 °C.

### 2.3 General Procedure for Suzuki–Miyaura Cross-Coupling Reactions

The BNP@SiO<sub>2</sub>(CH<sub>2</sub>)<sub>3</sub>NH-CC-AMP-Pd (0) (0.01 g of catalyst containing 0.0142 mmol of Pd) was dispersed in EtOH/H<sub>2</sub>O (1:1) and ArX (1.2 mmol), ArB(OH)<sub>2</sub> (1 mmol) and KOH (2 mmol) were added consecutively. Then, the mixture was stirred at 80 °C for an appropriate period of time (Table 2). After completion of the reaction, as monitored by TLC (n-hexane/EtOAc, 90:10), the catalyst was separated from the reaction mixture by centrifugation and washed by ethanol. After that, the organic solvent was evaporated under vacuum with a rotary evaporator to obtain pure biphenyl derivatives in excellent yields. Then, further purification was carried out in ethyl acetate-hexane solvents.

### 2.4 General Procedure for Mizoroki–Heck Cross-Coupling Reactions

In a round bottom flask, a mixture of aryl halide (1 mmol), styrene (1.2 mmol) and Et<sub>3</sub>N (3 mmol) and catalyst (0.01 g of catalyst containing 0.0142 mmol of Pd) was added and heated at 100 °C in solvent-free conditions for a specific time (Table 4). The progress of the reaction was indicated by TLC and when the reaction was completed, (10 mL) ethyl

acetate was added to the mixture. The catalyst was isolated by centrifugation and washed by ethanol. After evaporation of the organic solvent, the desired product was obtained and further purification in *n*-hexane–ethyl acetate was performed to produce the pure product in excellent yield.

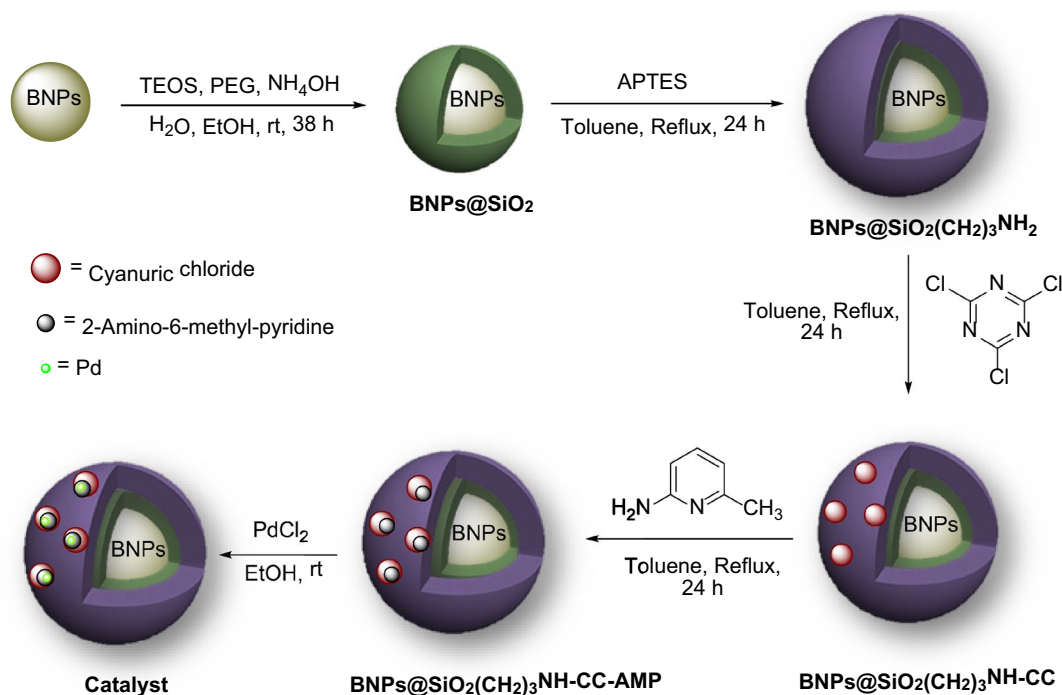
## 3 Results and Discussion

The preparation strategy of the BNP@SiO<sub>2</sub>(CH<sub>2</sub>)<sub>3</sub>NH-CC-AMP-Pd (0) was summarized in Scheme 2.

### 3.1 Characterization of the Catalyst

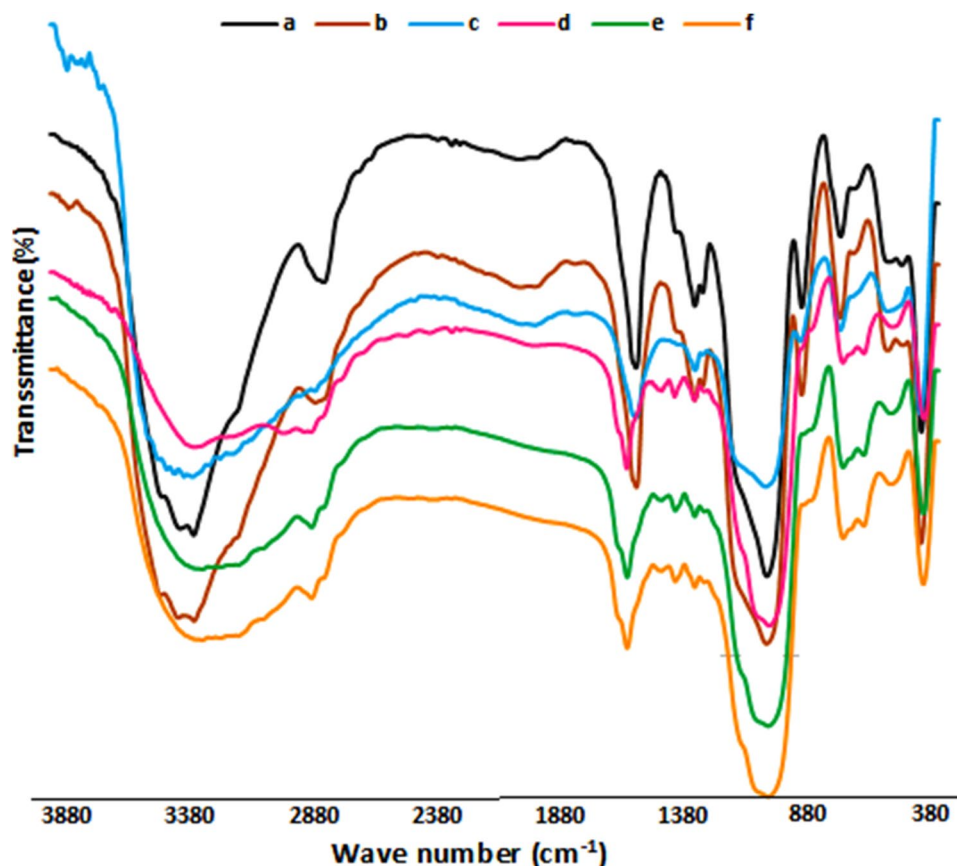
The synthesized catalyst was analyzed through some characterization techniques including FT-IR, XRD, FESEM, TEM, EDX, mapping, TGA, XPS and ICP.

FT-IR confirms the modification of the BNP surface. Figure 1a shows, strong absorption bands at 3383.34 and 3609.24 cm<sup>-1</sup> (black line) correspond to stretching frequencies of the O–H bonds of BNPs. Three bands at 801.56, 747.74 and 467.92 cm<sup>-1</sup> were related to Al–O vibrations [46]. Additionally, two absorption bands at 1035.12 and 1237.25 cm<sup>-1</sup> are related to the symmetrical bending vibrations of hydrogen bonds OH...OH. It should be noted that vibration of nitrate impurity was indicated at 1630.03 cm<sup>-1</sup>



Scheme 2 Synthetic steps of the catalyst

**Fig. 1** a FT-IR spectrum of BNPs b BNPs@SiO<sub>2</sub> c BNPs@SiO<sub>2</sub>(CH<sub>2</sub>)<sub>3</sub>NH<sub>2</sub> d BNPs@SiO<sub>2</sub>(CH<sub>2</sub>)<sub>3</sub>NH-CC e BNPs@SiO<sub>2</sub>(CH<sub>2</sub>)<sub>3</sub>NH-CC-AMP and f BNPs@SiO<sub>2</sub>(CH<sub>2</sub>)<sub>3</sub>NH-CC-AMP-Pd (0)



[47]. In FT-IR of BNPs@SiO<sub>2</sub> (Fig. 1b), Al-O absorptions are appeared at 473.01, 611.32 and 795.41 cm<sup>-1</sup>, also, two bands at 3411.80 and 3551.52 are attributed to the O-H stretching frequencies. After the connection of APTES to the surface of BNPs@SiO<sub>2</sub>, vibration frequencies of the Al-O are appeared at 467.34, 596.30 and 801.56 cm<sup>-1</sup>, which shift slightly with respect to the boehmite and boehmite silica FT-IR spectra, indicating a successful modification of the boehmite surface (Fig. 1c).

In the next step, cyanuric chloride was placed on the nano-catalyst surface (Fig. 1d) and in the FT-IR spectrum several frequencies are observed such as Al-O stretching absorptions (400 to 790 cm<sup>-1</sup>), two bending vibrations of hydrogen bonds OH...OH (1098.61 and 1175.13 cm<sup>-1</sup>), C=N absorption peak (1522.40 cm<sup>-1</sup>) and bending frequency of N-H (1662.20 cm<sup>-1</sup>).

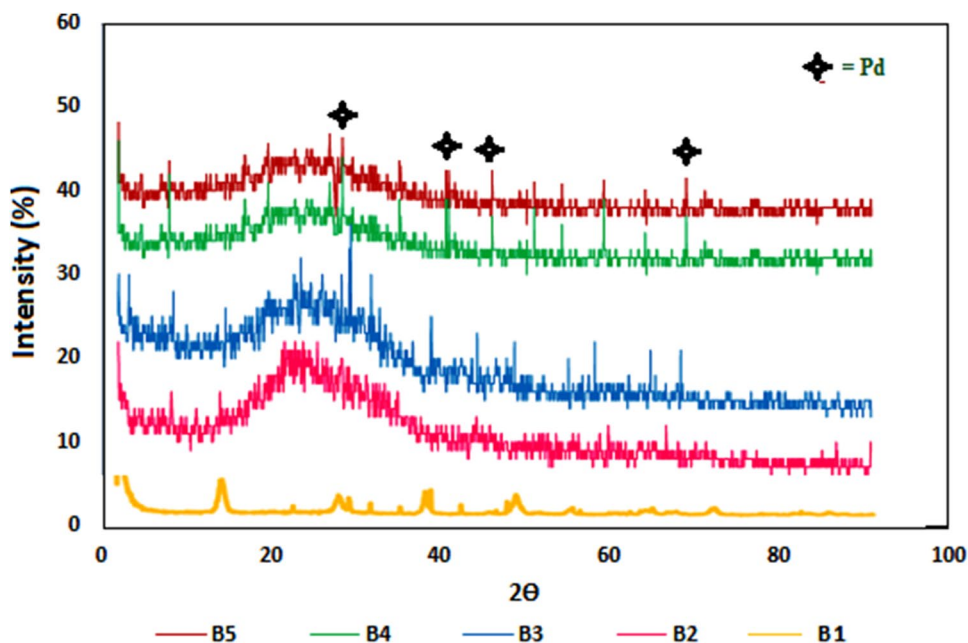
In the FT-IR spectrum of BNPs@SiO<sub>2</sub>(CH<sub>2</sub>)<sub>3</sub>NH-CC-AMP (Fig. 1e), the peak of the hydrogen bonding of hydroxyl groups is due to the connection of a cyanuric chloride and 2 amino-6-methyl-pyridine on the boehmite surface shifts to region 1074.71 cm<sup>-1</sup>. Absorption band appeared at 1661.30 cm<sup>-1</sup> ascribe to N-H bending vibration. Moreover, the C=N stretching frequency is appeared at 1642.32 cm<sup>-1</sup> which is buried beneath the bending vibration of the N-H. Also, the characteristic bands for C-H aliphatic bond are

appeared at ~1465 cm<sup>-1</sup> and vibration band at 3416.63 cm<sup>-1</sup> belongs to the amino group attached to the pyridine ring [26].

As can be seen from FT-IR spectrum of the final catalyst (Fig. 1f), the absorption band associated with N-H vibration shifts to a lower frequency (3383.16 cm<sup>-1</sup>) due to the connection to the palladium. The position of the hydrogen bonds transfers to higher frequencies (1107.30 cm<sup>-1</sup> and 1199.51 cm<sup>-1</sup>) and the location of bending frequency of N-H bond moves to a lower frequency, as well as the binding of palladium to the surface of the nano-catalyst is confirmed.

The crystalline structure of boehmite NPs: B1, BNPs@SiO<sub>2</sub>: B2, BNPs@SiO<sub>2</sub>(CH<sub>2</sub>)<sub>3</sub>NH-CC-AMP: B3 and BNPs@SiO<sub>2</sub>(CH<sub>2</sub>)<sub>3</sub>NH-CC-AMP-Pd (0): B4 and reused catalyst after 7th load: B5 was confirmed by the XRD technique (Fig. 2). In the XRD pattern you can see several peaks at 2θ = 14.52° (0 2 0), 28.18° (0 2 1), 31.88° (1 1 0), 38.35° (1 1 0), 45.83° (1 3 1), 48.38° (1 5 0), 49.02° (0 0 2), 51.55° (0 2 2), 55.16° (1 5 1), 58.28° (0 4 2), 64.85° (2 0 0), 65.18° (0 0 2), 68.12° (0 6 2), 72.19° (2 2 1) and 86.07° (1 1 3) which confirms the orthorhombic structure for boehmite. It should be noted that after attaching the silica layer (TEOS) to the boehmite surface, the X-ray spectrum widens especially at 2θ = 20-30°, also some peaks shift to lower or higher frequencies and the intensity of some peaks decreases

**Fig. 2** XRD patterns of **B1** BNP, **B2** BNP@SiO<sub>2</sub>, **B3** BNP@SiO<sub>2</sub>(CH<sub>2</sub>)<sub>3</sub>NH-CC-AMP, **B4** BNP@SiO<sub>2</sub>(CH<sub>2</sub>)<sub>3</sub>NH-CC-AMP-Pd (0) and **B5** reused catalyst after 7th run



[13]. In the BNP@SiO<sub>2</sub>(CH<sub>2</sub>)<sub>3</sub>NH-CC-AMP XRD pattern: B3, peaks were shifted to the boehmite XRD spectrum, indicating a ligand connection to the boehmite. In addition, new peaks in regions  $2\theta = 8.60^\circ$ ,  $25.50^\circ$  and  $65.07^\circ$  are probably related to the ligand bonding on the boehmite surface. Also, from the XRD survey of the catalyst: B4, the presence of palladium (0) on boehmite was confirmed, and peaks in the locations of  $2\theta = 28.475^\circ$  (1 1 1),  $40.67^\circ$  (2 0 0),  $46.145^\circ$  and  $68.8^\circ$  (3 3 1) respectively, are related to Pd (0) (space

group: *Fm* – 3 *m*, JCPDS Card No. 00-001-1201) [9, 48]. As B5 XRD spectrum indicates, the structure of the reused catalyst is indeed similar to the fresh catalyst and just the peak intensity has been slightly reduced.

Subsequently, using the FESEM technique, particle size and morphology of BNP@SiO<sub>2</sub>(CH<sub>2</sub>)<sub>3</sub>NH-CC-AMP-Pd (0) were investigated. According to the (Fig. 3), the prepared nano-catalyst showed appropriate dispersity with an average

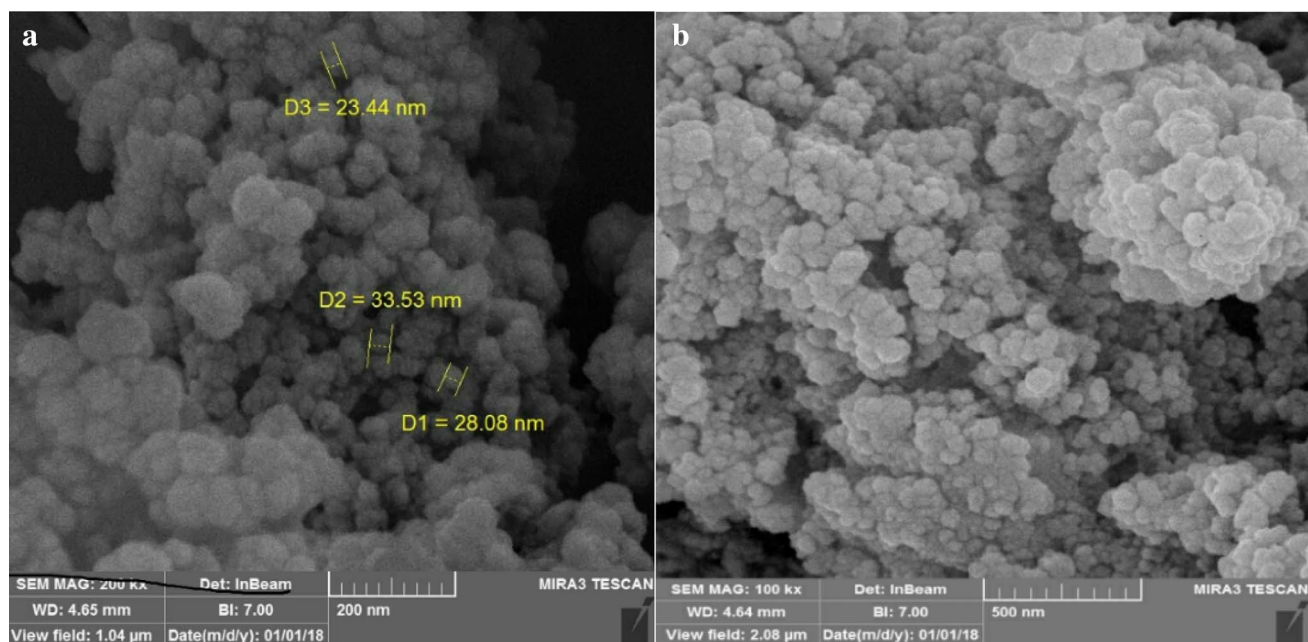


**Fig. 3** FESEM Images of the catalyst with different magnifications

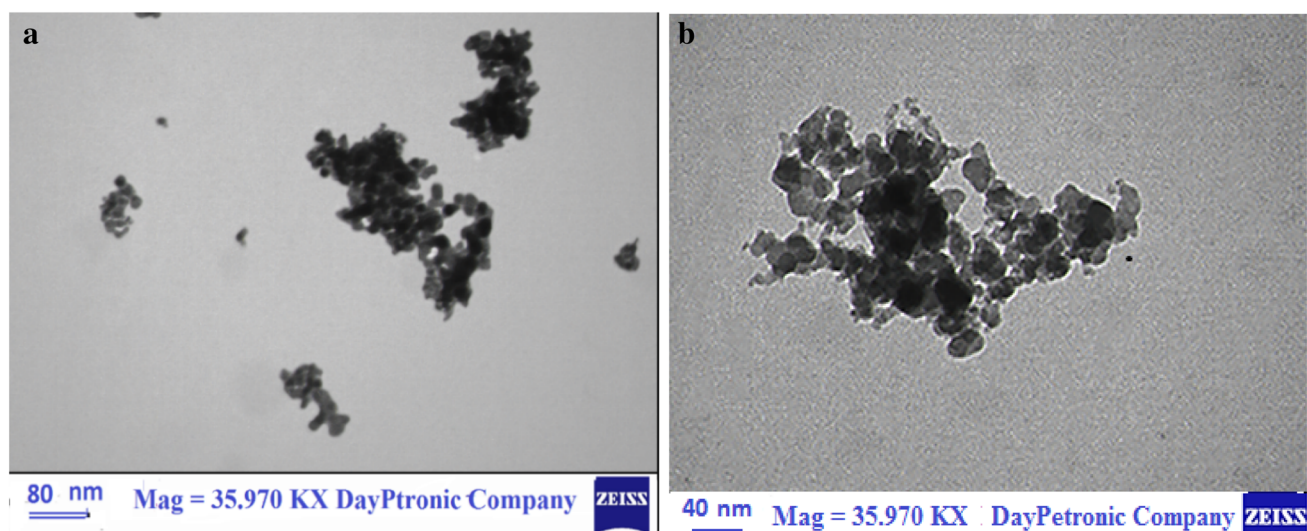


**Fig. 4** TEM images and particle size distribution histogram of the BNP@SiO<sub>2</sub>(CH<sub>2</sub>)<sub>3</sub>NH-CC-AMP-Pd (0)

size of 20–35 nm, and the shape of the particles is almost spherical.

As can be seen in Fig. 4, TEM reveals well dispersed Pd-NPs have an irregular geometric shape and a small amount of accumulation can be seen. Also, the particle size according to the particle size distribution histogram is between 5 and 40 nm, and the particles with the size of 20–30 nm have the largest number.

To investigate all types of elements in the fresh catalyst, the energy-dispersive X-ray (EDX) spectrum was used, the EDX results confirm the presence of palladium A%: 2.82 on the surface of the BNP- BNP@SiO<sub>2</sub>(CH<sub>2</sub>)<sub>3</sub>NH-CC-AMP-Pd (0) (Fig. 5). And also the atomic percent of the elements are C (A%: 22.93), Al (A%: 10.87), O (A%: 34.67) N (A%: 6.60) and Si (A%: 22.11).

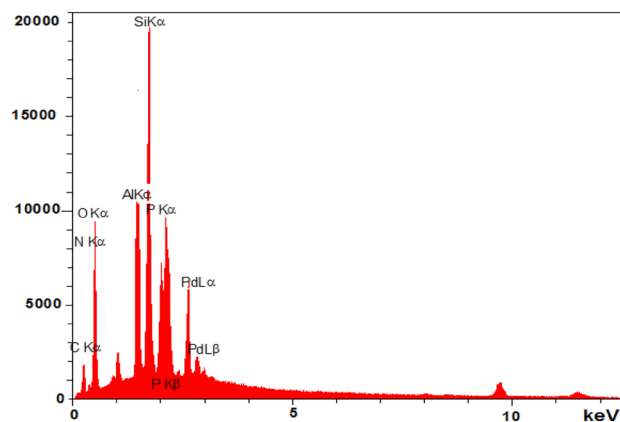


**Fig. 5** EDX pattern of BNP@SiO<sub>2</sub>(CH<sub>2</sub>)<sub>3</sub>NH-CC-AMP-Pd (0)

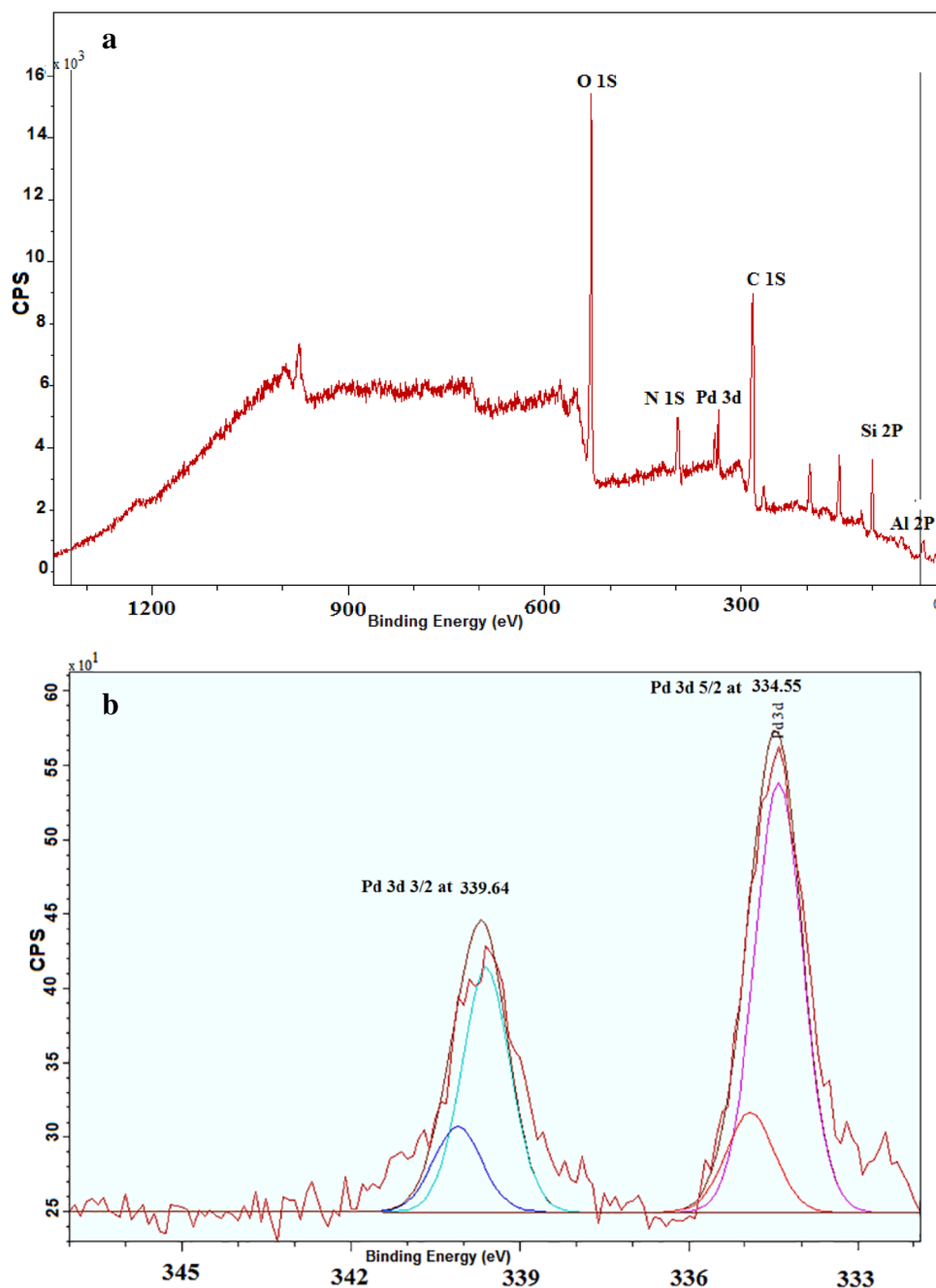
The XPS analysis allows us to obtain information about the elements in the sample, the chemical environment surrounding them and the oxidation state of the elements. The XPS survey of the BNP<sub>s</sub>@SiO<sub>2</sub>(CH<sub>2</sub>)<sub>3</sub>NH-CC-AMP-Pd (0) perfectly confirms the presence of palladium, and the high-resolution spectrum shows that palladium is Pd (0), with a doublet (Pd 3d<sub>5/2</sub> at 334.55 eV and Pd 3d<sub>3/2</sub> at 339.64 eV.) (Fig. 6a, b) [13, 49].

It should be noted that nitrogenous ligands, increase the dispersion and stability of the metal nanoparticles [46]. Furthermore, it is demonstrated that PdCl<sub>2</sub> can be reduced

to Pd NPs using EtOH and nitrogenous ligands as reducing agents [50–52].

The synthesis of the Pd (0) catalyst was initially monitored by UV–Visible spectroscopy (Fig. 7). In the UV–Visible spectrum of the PdCl<sub>2</sub> solution, the observed peak at 425 nm shows the presence of palladium (II) ions. During the attaching of Pd NPs to the surface of BNP<sub>s</sub>@SiO<sub>2</sub>(CH<sub>2</sub>)<sub>3</sub>NH-CC-AMP, the information obtained from the UV spectrum confirms the conversion of palladium (II) to metallic palladium by removing the peak in region 425 [39]. Another way of confirming the conversion of Pd (II)

**Fig. 6** **a** XPS survey of BNP<sub>s</sub>@SiO<sub>2</sub>(CH<sub>2</sub>)<sub>3</sub>NH-CC-AMP-Pd (0) **b** Pd 3d high resolution XPS spectrum of BNP<sub>s</sub>@SiO<sub>2</sub>(CH<sub>2</sub>)<sub>3</sub>NH-CC-AMP-Pd (0)



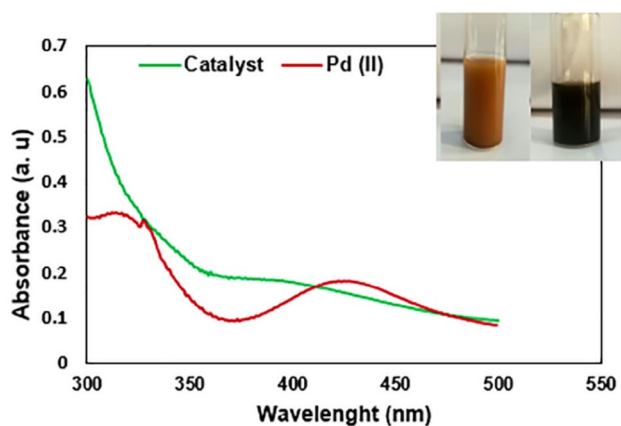


Fig. 7 UV-Vis spectrum of catalyst and  $\text{PdCl}_2$

to Pd (0) is colour change of palladium solution, so that the palladium colour changed from brown to black during the catalyst synthesis within 12 h (Fig. 7) [11, 43].

The presence of functional groups attached to the catalyst surface can be checked using the TGA technique (Fig. 8). According to literature, boehmite is stable to 400 °C and maintains more than 90% of its weight [5]. The TGA curve in Fig. 8 exhibits that the thermal decomposition and weight loss of  $\text{BNPs}@ \text{SiO}_2(\text{CH}_2)_3\text{NH-CC-AMP-Pd (0)}$  occurring in four steps. In the first step, 2.84% weight loss occurs at 50 to 150 °C, which is related to the loss of water or organic solvent. Also, weight loss in the range of 200 to 560 °C which is ascribed to the thermal decomposition of organic compounds like cyanuric chloride and 2-amino-6-methylpyridine from the catalyst surface. The fourth weight loss occurring after 560 °C is related to the boehmite crystalline structure change. As shown in TGA curve,  $\text{BNPs}@ \text{SiO}_2(\text{CH}_2)_3\text{NH-CC-AMP-Pd (0)}$  was stable even at 200 °C.

Fig. 8 TGA curve of  $\text{BNPs}@ \text{SiO}_2(\text{CH}_2)_3\text{NH-CC-AMP-Pd (0)}$

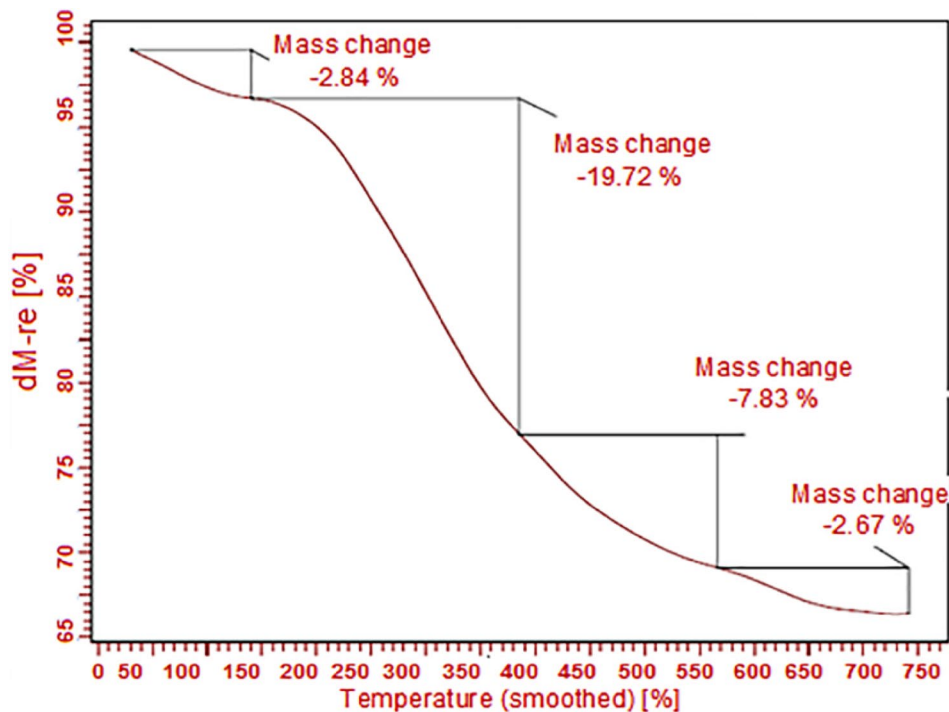
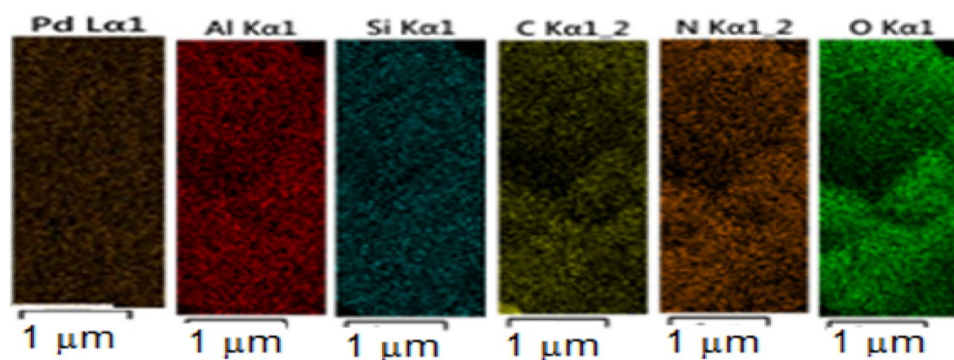


Fig. 9 Mapping analysis of  $\text{BNPs}@ \text{SiO}_2(\text{CH}_2)_3\text{NH-CC-AMP-Pd (0)}$



Another technique that used to confirm the existence of the elements in the catalyst structure is mapping technique, that well displays the distribution of all elements in the BNP@SiO<sub>2</sub>(CH<sub>2</sub>)<sub>3</sub>-NH-CC-AMP-Pd (0) structure (Fig. 9).

### 3.2 Catalytic Studies

The catalytic activity of the BNP@SiO<sub>2</sub>(CH<sub>2</sub>)<sub>3</sub>-NH-CC-AMP-Pd (0) was evaluated in the carbon–carbon coupling reactions (Suzuki–Miyaura, Mizoroki–Heck reactions). To optimize the Suzuki–Miyaura reaction conditions, we investigated various factors such as solvent, different catalyst amounts, various bases and temperature effect on the reaction. Initially, we went through different solvents and according to the results, the best solvents for reaction between iodobenzene and phenylboronic acid were much more polar solvents such as DMF and H<sub>2</sub>O, EtOH. But, we chose H<sub>2</sub>O, EtOH as solvent for this reaction because it is green, safe and environmentally friendly (Table 1, entries 4,11). Further experiments were also carried out to obtain the optimum ratio of reactants, such as the study

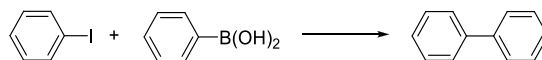
of different ratios of iodobenzene to phenylboronic acid and iodobenzene to base. The results of these surveys are shown in Table 1 (entries 13–18).

In this work, the BNPs were coated with a layer of silica using tetraethyl orthosilicate (TEOS) to increase thermal stability, to provide further reaction sites for further functionalization, to reduce particle aggregation, to make easy surface modification and to make easy control of interparticle interactions, both in solution and within structures. Finally, and most importantly, the silica surface is terminated by abundant silanol groups (–Si–OH), which can react with various coupling agents [16, 53].

On the other hand, BNP-APTES-CC-AMP-Pd (0) was synthesized with directly attaching of the APTES to the BNPs surface and in this case the yield of Suzuki reaction is lower than BNP@SiO<sub>2</sub>(CH<sub>2</sub>)<sub>3</sub>-NH-CC-AMP-Pd (0), because the number of hydroxyl groups and ligand-modified sites on the surface of the boehmite are lower than BNP@SiO<sub>2</sub>(CH<sub>2</sub>)<sub>3</sub>-NH-CC-AMP-Pd (0) (Table 1, entry 19).

Under optimized conditions, our attention was focused on checking out the scope of Suzuki reaction using different

**Table 1** Optimization of conditions in the Suzuki-Miyaura coupling reaction

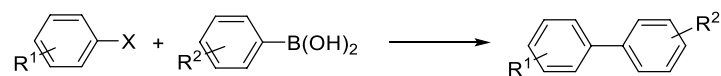


Entry	Cat. (mol%)	Base	Iodobenzene/phenylboronic	Iodobenzene/base	Solvent	T (°C)	Yield (%) <sup>a</sup>
1	1.42	–	1.2/1	1.2/2	EtOH–H <sub>2</sub> O	80	–
2	0.56	KOH	1.2/1	1.2/2	EtOH–H <sub>2</sub> O	80	35
3	0.99	KOH	1.2/1	1.2/2	EtOH–H <sub>2</sub> O	80	70
4	1.42	KOH	1.2/1	1.2/2	EtOH–H <sub>2</sub> O	80	96
5	2.13	KOH	1.2/1	1.2/2	EtOH–H <sub>2</sub> O	80	98
6	1.42	K <sub>2</sub> CO <sub>3</sub>	1.2/1	1.2/2	EtOH–H <sub>2</sub> O	80	65
7	1.42	NEt <sub>3</sub>	1.2/1	1.2/2	EtOH–H <sub>2</sub> O	80	45
8	1.42	Na <sub>2</sub> CO <sub>3</sub>	1.2/1	1.2/2	EtOH–H <sub>2</sub> O	80	60
9	1.42	KOH	1.2/1	1.2/2	EtOH–H <sub>2</sub> O	70	80
10	1.42	KOH	1.2/1	1.2/2	DMF	110	95
11	1.42	KOH	1.2/1	1.2/2	H <sub>2</sub> O	80	30
12	1.42	KOH	1.2/1	1.2/2	EtOH	70	70
13	1.42	KOH	1/1	1/2	EtOH–H <sub>2</sub> O	80	78
14	1.42	KOH	1.1/1	1.1/2	EtOH–H <sub>2</sub> O	80	87
15	1.42	KOH	1.3/1	1.3/2	EtOH–H <sub>2</sub> O	80	96
16	1.42	KOH	1/1	1/3	EtOH–H <sub>2</sub> O	80	88
17	1.42	KOH	1/1	1/4	EtOH–H <sub>2</sub> O	80	91
18	1.42	KOH	1/1	1/5	EtOH–H <sub>2</sub> O	80	94
19	Cat.*	KOH	1.2/1	1.2/2	EtOH–H <sub>2</sub> O	80	70

Reaction conditions: Iodobenzene (1.2 mmol), phenylboronic acid (1 mmol), base (2 mmol), solvent (3 mL), 1 h

<sup>a</sup>Isolated yields

\*BNP-APTES-CC-AMP-Pd (0)

**Table 2** Suzuki–Miyaura coupling reactions of aryl halides with aryl boronic acid

Entry	X	R <sup>1</sup>	R <sup>2</sup>	Time (min)	Yield (%) <sup>a</sup>	TON <sup>b</sup>	M.p [Refs]
1	I	H	H	40	96	67.60	66 [54]
2	I	4-CH <sub>3</sub>	H	48	97	68.30	43–44 [54]
3	I	4-NO <sub>2</sub>	H	35	94	66.19	114 [55]
4	I	H	4-CH <sub>3</sub>	37	98	69.01	42–44 [55]
5	I	4-NO <sub>2</sub>	3-NO <sub>2</sub>	65	96	67.60	182–184 [56]
6	Br	H	H	40	94	66.19	65–67 [54]
7	Br	H	4-OCH <sub>3</sub>	40	95	66.90	85–88 [55]
8	Br	H	4-F	55	90	63.38	74–76 [57]
9	I	4-MeCO	4-OCH <sub>3</sub>	35	95	66.90	147–148 [54]
10	Br	4-CH <sub>3</sub>	H	45	98	69.01	45 [55]
11	Cl	H	H	100	80	56.33	65 [54]
12	Cl	4-NO <sub>2</sub>	H	60	95	66.90	114 [55]

Reaction conditions: Aryl halide (1.2 mmol), aryl boronic acid (1 mmol), KOH (2 mmol), EtOH/H<sub>2</sub>O (3 mL), catalyst (0.01 g; 0.0142 mmol)

<sup>a</sup>Isolated yields

<sup>b</sup>TON = mmol product/mmol Pd

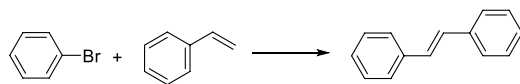
substituted aryl halides with aryl boronic acids and the obtained results are summarized in Table 2. It was found that, aryl boronic acids with both electron-withdrawing and electron-donating groups reacted well with different aryl halides to give the desired products in excellent yields. Based on the obtained evidences from Table 2, aryl boronic acids with electron-rich groups in the para situation increase the rate of the reaction by increasing the nucleophilicity of aryl boronic acid. Aryl boronic acids containing electron-withdrawing groups in the para and meta positions have lower reaction rates. In addition, substituted aryl iodides containing electron-withdrawing groups increase the rate of the reactions, whereas the electron donating groups show lower activities. As expected, the Suzuki reaction rate is lower with aryl chloride and the reaction time is longer, but the reaction rate with 4-nitro-1-chlorobenzene is similar to that of iodobenzene and is higher than chlorobenzene (Table 2, entries 11,12).

In the next step, we surveyed the catalytic efficiency of BNPs@SiO<sub>2</sub>(CH<sub>2</sub>)<sub>3</sub>NH-CC-AMP-Pd (0) for the Mizoroki–Heck C–C coupling reaction. For this regard, to find the best reaction conditions for the Mizoroki–Heck C–C coupling reaction, model reaction between styrene and bromobenzene was investigated in the presence of different amount of the catalyst, different bases such as KOH, K<sub>2</sub>CO<sub>3</sub>, NEt<sub>3</sub>, solvents like H<sub>2</sub>O, EtOH, DMF and solvent-free conditions at 100 °C (Table 3).

Initially, the reaction was performed in the absence of base and no product was observed (Table 3, entry 1). According to the findings, the lowest time and the highest yield were obtained in the presence of 0.01 g of the catalyst (1.42 mol%), NEt<sub>3</sub> (3 mmol) as base and solvent-free conditions (Table 3, entry 4). Higher amount of catalyst did not lead to significant change in the yield of reaction (Table 3, entry 5).

More investigations were carried out to obtain the best ratio of reactants. In this regard, different ratios of bromobenzene/base and bromobenzene/styrene were investigated in the solvent-free conditions. The findings are summarized in Table 3 (entries 11–16). We also surveyed the model reaction under the optimized conditions in the presence of BNPs-APTES-CC-AMP-Pd (0) instead of BNPs@SiO<sub>2</sub>(CH<sub>2</sub>)<sub>3</sub>NH-CC-AMP-Pd (0). As can you see, in this case, the yield is lower than before case (Table 3, entry 17).

With this methodology in hand, a variety of aryl bromides, chlorides and iodides have been reacted with styrenes in mostly excellent yields (Table 4). The speed and efficiency of the reaction in the Heck reaction depend on the different halogen types. It should be noted, in the presence of aryl bromides and aryl chlorides the yields of products are lower than that of aryl iodides (Table 4, entries 1,3,8). The electronic effects of aryl halides having both electron with-drawing and electron donor groups in para position are almost identical in the Heck reaction.

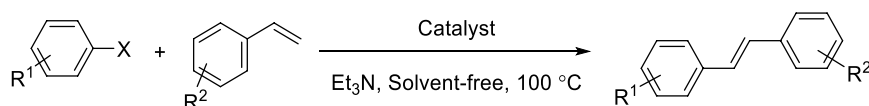
**Table 3** Optimization of reaction conditions

Entry	Catalyst (mol%)	Base	Bromobenzene/ styrene	Bromobenzene/base	Solvent	Yield (%) <sup>a</sup>
1	–	NEt <sub>3</sub>	1/1.2	1/3	No solvent	0
2	0.56	NEt <sub>3</sub>	1/1.2	1/3	No solvent	30
3	0.99	NEt <sub>3</sub>	1/1.2	1/3	No solvent	75
4	1.42	NEt <sub>3</sub>	1/1.2	1/3	No solvent	96
5	2.13	NEt <sub>3</sub>	1/1.2	1/3	No solvent	97
6	1.42	K <sub>2</sub> CO <sub>3</sub>	1/1.2	1/3	No solvent	70
7	1.42	KOH	1/1.2	1/3	No solvent	75
8	1.42	NEt <sub>3</sub>	1/1.2	1/3	DMF	80
9	1.42	NEt <sub>3</sub>	1/1.2	1/3	H <sub>2</sub> O	60
10	1.42	NEt <sub>3</sub>	1/1.2	1/3	EtOH	70
11	1.42	NEt <sub>3</sub>	1/1	1/3	No solvent	80
12	1.42	NEt <sub>3</sub>	1/1.1	1/3	No solvent	89
13	1.42	NEt <sub>3</sub>	1/1.3	-1/3	No solvent	96
14	1.42	NEt <sub>3</sub>	1/1.2	1/2	No solvent	84
15	1.42	NEt <sub>3</sub>	1/1.2	1/4	No solvent	96
16	1.42	NEt <sub>3</sub>	1/1.2	1/5	No solvent	97
17	1.42*	NEt <sub>3</sub>	1/1.2	1/3	No solvent	79

Reaction conditions: Bromobenzene (1 mmol), styrene (1.2 mmol), base (3 mmol), solvent (3 mL), 100 °C, 1 h

<sup>a</sup>Isolated yields

\*Catalyst: BNPs-APTES-CC-AMP-Pd (0)

**Table 4** Coupling reactions of aryl halides with styrene

Entry	X	R <sup>1</sup>	R <sup>2</sup>	Time (h)	Yield (%) <sup>a</sup>	TON <sup>b</sup>	M.p [Refs]
1	I	H	H	1	96	67.60	117–120 [58]
2	I	4-NO <sub>2</sub>	H	1	95	66.90	150–153 [58]
3	Br	H	H	2	92	64.78	121–123 [58]
4	Br	4-NO <sub>2</sub>	H	2	90	63.38	150–152 [58]
5	Br	4-CH <sub>3</sub>	H	2	92	64.78	116 [59]
6	Cl	4-NO <sub>2</sub>	H	1.5	94	66.19	150–152 [59]
7	I	H	2-CH <sub>3</sub>	3	80	56.33	Oil [60]
8	Cl	H	H	2.5	75	52.81	121–123 [59]

Reaction conditions: Aryl halide (1 mmol), styrene (1.2 mmol), NEt<sub>3</sub> (3 mmol), catalyst (0.01 g: 0.0142 mmol), under solvent-free, 100 °C

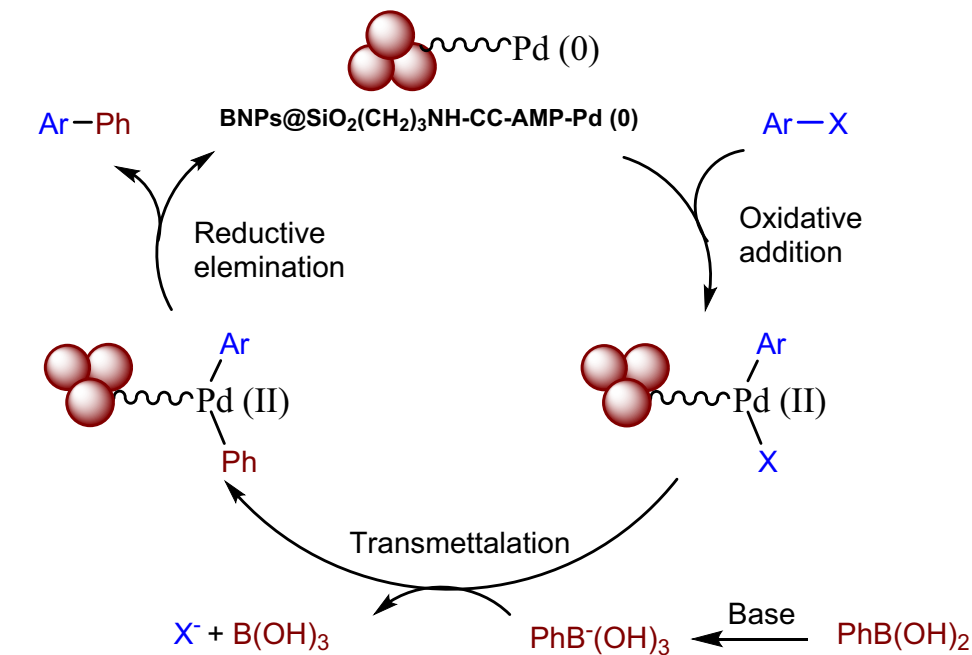
<sup>a</sup>Isolated yield

<sup>b</sup>TON = mmol product/mmol Pd

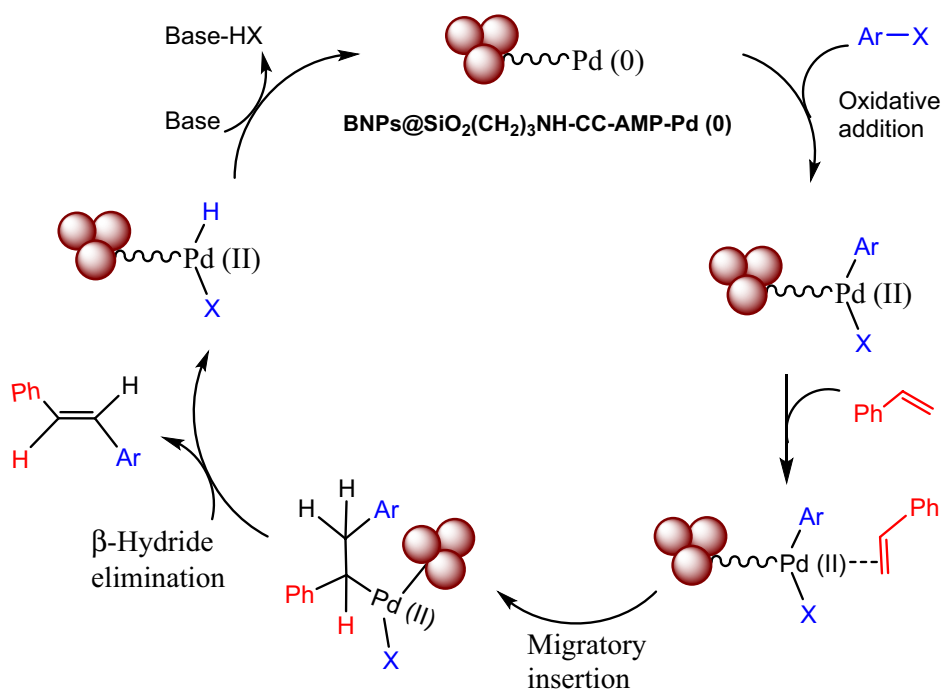
In addition, all three halides react well but the yields for iodobenzene are higher than bromobenzene and chlorobenzene. Also, in general, styrene compounds with electron donor substituents in the para position react faster than

styrene derivatives with electron poor groups. The substituents in the ortho position of the styrene ring decrease the reaction speed and efficiency due to the space barrier of these substituents (Table 4, entry 7). It is of interest to

**Scheme 3** Mechanism for **a** Suzuki–Miyaura and **b** Mizoroki–Heck reactions in the presence of  $\text{BNPs}@SiO_2(CH_2)_3NH-CC-AMP-Pd(0)$

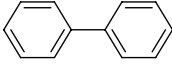
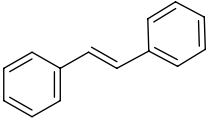


**a** Suzuki–Miyaura reaction mechanism



**b** Mizoroki–Heck reaction mechanism

**Table 5** Comparison of the efficiency of the synthesized catalyst with some previously reported catalysts in cross-coupling reactions

Entry	Product	Conditions	Mol % or g	Time (h)	Yield (%)
1		Pd-MPA@MCM-41, PEG, 100 °C, K <sub>2</sub> CO <sub>3</sub> [62]	1.7 mol%	2	95
2		FMNPs@TPy-Pd, Na <sub>2</sub> CO <sub>3</sub> , reflux, SDS micellar solution [63]	0.1 g	0.6	97
3		GO-CPTMS@Pd-TKHPP, air EtOH:H <sub>2</sub> O, K <sub>2</sub> CO <sub>3</sub> , 80 °C [48]	10 mol%	0.25	99
4		Pd-isatin-boehmite, K <sub>2</sub> CO <sub>3</sub> , PEG, 80 °C [64]	0.01 g	0.83	97
5		CA/Pd(0), K <sub>2</sub> CO <sub>3</sub> , 100 °C, H <sub>2</sub> O [65]	0.5 mol%	2	94
6		GO/NHC-Pd, Na <sub>3</sub> PO <sub>4</sub> ·12H <sub>2</sub> O, H <sub>2</sub> O, 100 °C [66]	1 mo%	6	91.6
7		This work	1.42 mol%	0.66	96
8		GO-CPTMS@Pd-TKHPP, air, DMF, K <sub>2</sub> CO <sub>3</sub> , 120 °C [48]	10 mol%	0.33	95
9		GO/NHC-Pd, Na <sub>3</sub> PO <sub>4</sub> ·12H <sub>2</sub> O, H <sub>2</sub> O, 100 °C [66]	1 mol%	12	55
10		FMNPs@TPy-Pd, Na <sub>2</sub> CO <sub>3</sub> , reflux, SDS micellar solution, 100 °C [63]	0.08 g	8	92
11		ERGO-Pd, NEt <sub>3</sub> , DMF, 120 °C [67]	0.3 mol%	2	91
12		TRGO-NPy-Pd, Na <sub>2</sub> CO <sub>3</sub> , DMF, 140 °C [68]	0.3 mol%	5	97
13		(1,4-C <sub>6</sub> H <sub>4</sub> )(GO-CPTMS@HPTPy-Pd-TPy) <sub>2</sub> , NEt <sub>3</sub> , 110 °C, solvent-free [52]	1.38 mol%	4	95
14		This work	1.42 mol%	1	96

**Table 6** Suzuki and Heck reactions catalyzed by recycled BNP<sub>s</sub>@SiO<sub>2</sub>(CH<sub>2</sub>)<sub>3</sub>NH-CC-AMP-Pd (0)

Entry	Suzuki yield (%)	Heck yield (%)
1	96	95
2	96	95
3	95	94
4	92	90
5	92	88
6	90	87
7	88	85

note that the reaction rate of styrene is higher with 4-nitro-1-chlorobenzene and the product is higher than that of chlorobenzene (Table 4, entries 6 and 8).

Possible mechanism for Suzuki and Heck cross-coupling reactions in the presence of BNP<sub>s</sub>@SiO<sub>2</sub>(CH<sub>2</sub>)<sub>3</sub>NH-CC-AMP-Pd (0) is outlined in Scheme 3 [61].

The efficiency of this synthesized nano-catalyst was compared with some of the palladium catalysts in Suzuki and Heck coupling reactions (Table 5). As can be seen from Table 5, the synthesized nano-boehmite is comparable and superior to some previously reported methods in terms of efficiency, yield and time.

### 3.3 Reusability of the Catalyst

Nowadays, one of the important issues in the field of nano-catalysts is their reusability, and for this purpose, the recyclability of the synthesized catalyst was investigated. The catalyst is easily separated from the reaction mixture by centrifugation and washed with ethanol and then with water. After drying, the catalyst was used in the reaction between phenylboronic acid and phenyl iodide under optimized reaction conditions and the product was 96% after 40 min. It is worth noting that recovered catalytic system is still more active and used for 7 consecutive times without any particular change in catalytic activity. The results for the seven repeat runs are presented in Table 6. Hg poisoning test, hot filtration method, ICP and SEM were used to confirm the recyclability of the catalyst.

### 3.4 Hg Poisoning Test

To carry out the Hg poisoning test, in a round bottom flask, a mixture of phenyl boronic acid (1 mmol), iodobenzene (1.2 mmol), KOH (2 mmol) and BNP<sub>s</sub>@

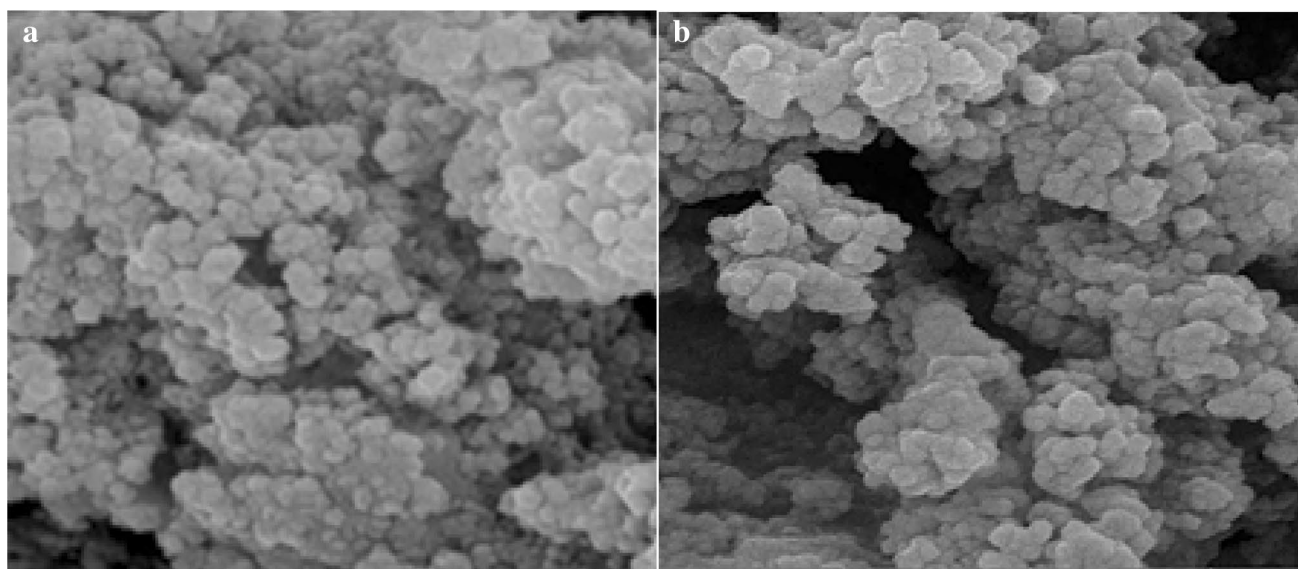


**Fig. 10** a SEM image after run 1 b SEM image after run 7

$\text{SiO}_2(\text{CH}_2)_3\text{NH-CC-AMP-Pd (0)}$  (0.01 g, 1.42 mol %) was heated at 80 °C for 20 min. The progress of the reaction was screened by TLC (yield 52%). After that, metallic mercury was added to the reaction mixture. Then, the reaction was continued for another 20 min under the optimized reaction conditions (yield 96%) and then the catalyst and the used mercury were separated from the reaction mixture. It should be noted that the used mercury was metallic and this result clearly indicated the leaching of palladium into the reaction medium is negligible [69].

### 3.5 Hot Filtration Test

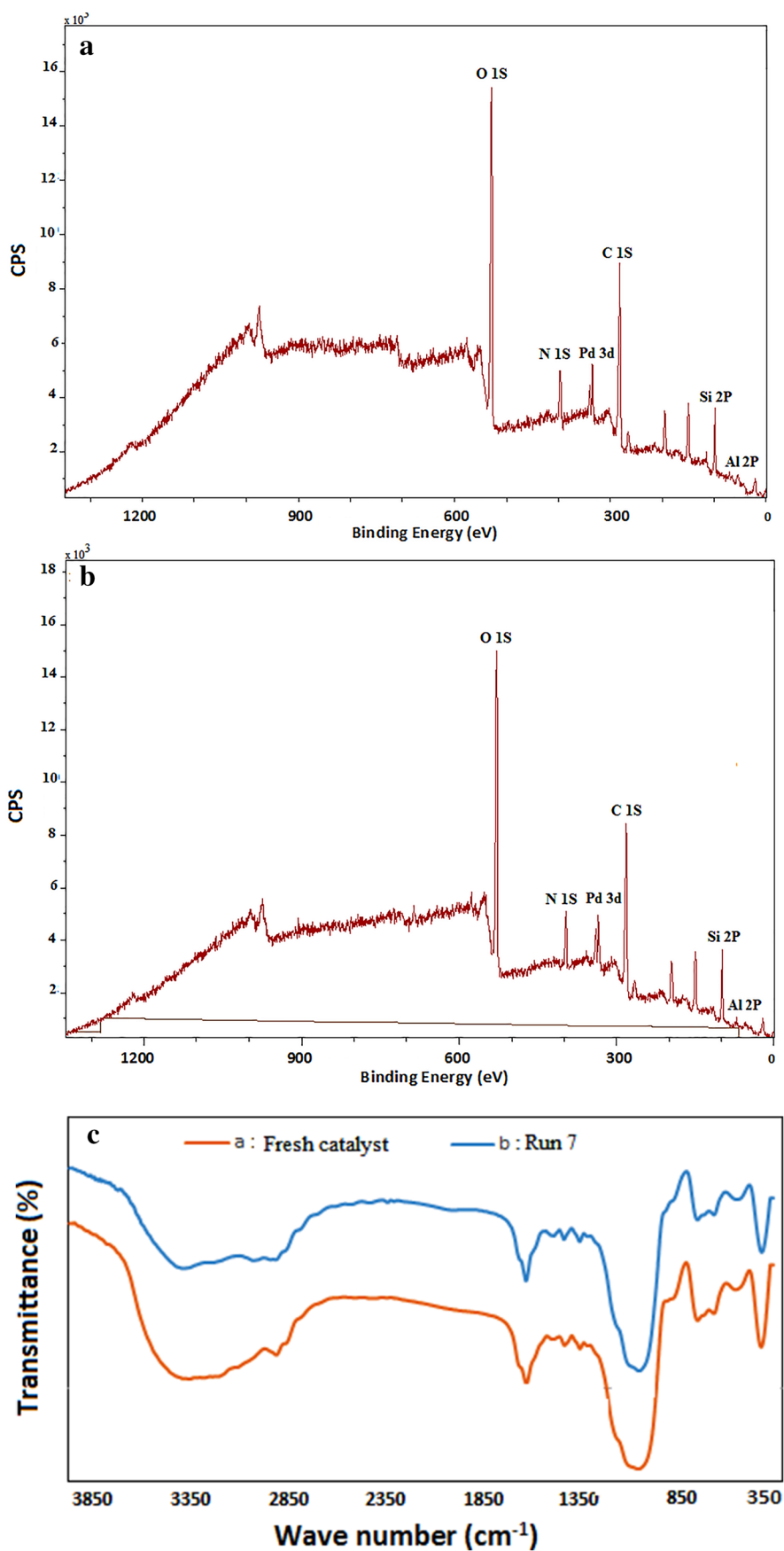
To perform hot-filtration test, the model reaction between phenylboronic acid and aryl iodide was performed under optimal reaction conditions. After the half-reaction time (30 min), the product was 50%. The catalyst was separated from the medium through filtration, and the reaction continued uninterrupted in the absence of the catalyst. After a long time, the reaction was not completed (yield: 52%), which indicates that palladium is not leached to the reaction medium. In addition, using the inductively coupled plasma (ICP) technique, the amount of palladium on the catalyst surface was 1.435 g/mmol and the amount of palladium on the catalyst surface after the seventh load was 1.296 g/mmol. With great pleasure, the obtained results indicate that the catalyst is stable and recyclable. As can be seen in Fig. 10, the morphology and catalyst structure are maintained after

the seventh load. Also, another analysis that confirms the stability and recyclability of the catalyst is the XPS analysis. As Fig. 11 illustrates, the catalyst XPS survey after the 7th load shows all the key elements and is quite similar to the fresh catalyst spectrum. In addition, in Fig. 11c, the FT-IR spectra of the fresh catalyst and the reused catalyst after the 7th run are compared, and the catalyst structure remains unchanged.

## 4 Conclusion

In summary, we successfully synthesized a well-designed heterogeneous catalyst through a fairly simple method and inexpensive material. As expected, the introduced nano-catalyst was effective and stable catalyst and catalyzed the carbon–carbon coupling reactions such as Suzuki–Miyaura and Mizoroki–Heck reactions, which are two important categories of organic reactions. Some of the salient features of this methodology are the thermal and mechanical stability of the catalyst, no need for a neutral atmosphere and hard conditions, high yields, good times, low palladium leaching (9.7%), and the use of catalyst for at least 7 times. We believe that this study will open new paths for the design and construction of new nano-catalysts. Further studies in this field are under study in our research laboratory, and similar works for the heterogenization of metal catalysts are underway.

**Fig. 11** **a** XPS survey of fresh catalyst and **b** XPS survey of catalyst after 7th run **c** FT-IR of fresh catalyst and reused catalyst after run 7th



**Acknowledgements** The authors gratefully acknowledge the financial support of this work by Razi University Research Council.

## References

- Jin R (2012) The impacts of nanotechnology on catalysis by precious metal nanoparticles. *Nanotechnol. Rev.* 1:31–56
- Buchwalter P, Rose J, Braunstein P (2014) Multimetallic catalysis based on heterometallic complexes and clusters. *Chem. Rev.* 115:28–126
- Gang L, Li Y, Qi Z, Fan H, Zhou Z, Chen R, Huang J (2016) Highly efficient palladium catalysts supported on nitrogen contained polymers for Suzuki-Miyaura reaction. *Catal. Commun.* 82:24–28
- Hajipour AR, Khorsandi Z, Farrokhpour H (2016) Regioselective Heck reaction catalyzed by Pd nanoparticles immobilized on DNA-modified MWCNTs. *RSC. Adv.* 6:59124–59130
- Hajjami M, Ghorbani-Choghamarani A, Ghafouri-Nejad R, Tahmasbi B (2016) Efficient preparation of boehmite silica dopamine sulfamic acid as a novel nanostructured compound and its application as a catalyst in some organic reactions. *New J. Chem.* 40:3066–3074
- Han L, Li H, Choi SJ, Park MS, Lee SM, Kim YJ, Park DW (2012) Ionic liquids grafted on carbon nanotubes as highly efficient heterogeneous catalysts for the synthesis of cyclic carbonates. *Appl. Catal. A* 429:67–72
- Sun Q, Zorin NA, Chen D, Chen M, Liu TX, Miyake J, Qian DJ (2010) Langmuir–Blodgett films of pyridyldithio-modified multi-walled carbon nanotubes as a support to immobilize hydrogenase. *Langmuir* 26:10259–10265
- Hajipour AR, Tadayoni NS, Khorsandi Z (2016) Magnetic iron oxide nanoparticles–N-heterocyclic carbene–palladium (II): a new, efficient and robust recyclable catalyst for Mizoroki-Heck and Suzuki-Miyaura coupling reactions. *Appl. Organomet. Chem.* 30:590–595
- Bahrami K, Khodamorady M (2018) Reusable BNPs-SiO<sub>2</sub>@(CH<sub>2</sub>)<sub>3</sub>NHSO<sub>3</sub>H-catalysed selective oxidation of sulfides to sulfones. *Appl. Organomet. Chem.* 32:e4553
- Bahrami K, Khodaei MM, Roostaei M (2014) The preparation and characterization of boehmite nanoparticles-TAPC: a tailored and reusable nanocatalyst for the synthesis of 12-aryl-8, 9, 10, 12-tetrahydrobenzo [a] xanthen-11-ones. *New J. Chem.* 38:5515–5520
- Khodamorady M, Bahrami K (2019) Fe<sub>3</sub>O<sub>4</sub>@BNPs-CPTMS-Chitosan-Pd (0) as an efficient and stable heterogeneous magnetic nanocatalyst for the chemoselective oxidation of alcohols and homoselective synthesis of 5-substituted 1H-tetrazoles. *Chemistryselect* 4:8183–8194
- Mirzaee M, Bahramian B, Amoli A (2015) Schiff base-functionalized boehmite nanoparticle-supported molybdenum and vanadium complexes: efficient catalysts for the epoxidation of alkenes. *Appl. Organomet. Chem.* 29:593–600
- Bahrami K, Khodamorady M (2019) Design of BNPs-TAPC Palladium Complex as a Reusable Heterogeneous Nanocatalyst for the O-Arylation of Phenols and N-Arylation of Amines. *Catal. Lett.* 149:688–698
- Gholivand MB, Malekzadeh G, Derakhshan AA (2014) Boehmite nanoparticle modified carbon paste electrode for determination of piroxicam. *Sens. Actuators B.* 201:378–386
- Granados-Correa F, Jiménez-Becerril J (2009) Chromium (VI) adsorption on boehmite. *J. Hazard. Mater.* 162:1178–1184
- Ghorbani-Choghamarani A, Tahmasbi B (2016) The first report on the preparation of boehmite silica sulfuric acid and its applications in some multicomponent organic reactions. *New J. Chem.* 40:1205–1212
- Rajabi L, Derakhshan AA (2010) Room temperature synthesis of boehmite and crystallization of nanoparticles: effect of concentration and ultrasound. *Sci. Adv. Mater.* 2:163–172
- Xu B, Wang J, Yu H, Gao H (2011) Large-scale synthesis of hierarchical flowerlike boehmite architectures. *J. Environ. Sci.* 23:S49–S52
- Tahmasbi B, Ghorbani-Choghamarani A (2017) Pd (0)-Arg-boehmite: as reusable and efficient nanocatalyst in Suzuki and Heck reactions. *Catal. Lett.* 147:649–662
- Kharissova OV, Kharisov BI, Jiménez-Pérez VM, Flores BM, Méndez UO (2013) Ultrasmall particles and nanocomposites: state of the art. *RSC. Adv.* 3:22648–22682
- Ramu VG, Bordoloi A, Nagaiah TC, Schuhmann W, Muhler M, Cabrele C (2012) Copper nanoparticles stabilized on nitrogen-doped carbon nanotubes as efficient and recyclable catalysts for alkyne/aldehyde/cyclic amine A<sub>3</sub>-type coupling reactions. *Appl. Catal. A* 431:88–94
- Pa A, Sevonkaev I, Bartling B, Rijssenbeek J, Goia DV (2014) Dipentaerythritol: a novel additive for the precipitation of dispersed Ni particles in polyols. *RSC. Adv.* 4:20909–20914
- Babu SG, Neelakandeswari N, Dharmaraj N, Jackson SD, Karvembu R (2013) Copper (II) oxide on aluminosilicate mediated Heck coupling of styrene with aryl halides in water. *RSC. Adv.* 3:7774–7781
- Hajipour AR, Azizi G (2013) Iron-catalyzed cross-coupling reaction: recyclable heterogeneous iron catalyst for selective olefination of aryl iodides in poly (ethylene glycol) medium. *Green Chem.* 15:1030–1034
- Ma Z, Guan Y, Liu H (2006) Superparamagnetic silica nanoparticles with immobilized metal affinity ligands for protein adsorption. *J. Magn. Mater.* 301:469–477
- Hajipour AR, Rezaei F, Khorsandi Z (2017) Pd/Cu-free Heck and Sonogashira cross-coupling reaction by Co nanoparticles immobilized on magnetic chitosan as reusable catalyst. *Green Chem.* 19:1353–1361
- Li-xia W, Zi-wei W, Guo-song W, Xiao-dong L, Jian-guo R (2010) Catalytic performance of chitosan-Schiff base supported Pd/Co bimetallic catalyst for acrylamide with phenyl halide. *Polym. Adv. Technol.* 21:244–249
- Khadir N, Tavakoli G, Assoud A, Bagherzadeh M, Boghaei DM (2016) Synthesis and crystal structures of a series of (μ-thiophenolato)(μ-pyrazolato-N, N') double bridged dipalladium (II) complexes and their application in Mizoroki-Heck reaction as highly efficient catalysts. *Inorg. Chim. Acta* 440:107–117
- Wang Y, Lu C, Yang G, Chen Z, Nie J (2017) A crosslinked bis (amino)-containing polymer as a remarkable support for heterogeneous palladium-catalyzed Suzuki-Miyaura reaction. *React. Funct. Polym.* 110:38–46
- Carini DJ, Duncia JV, Aldrich PE, Chiu AT, Johnson AL, Pierce ME, Wells GJ (1991) Nonpeptide angiotensin II receptor antagonists: the discovery of a series of N-(biphenylmethyl) imidazoles as potent, orally active antihypertensives. *J. Med. Chem.* 34:2525–2547
- Myers AG, Tom NJ, Fraley ME, Cohen SB, Madar DJ (1997) A convergent synthetic route to (+)-dynemicin A and analogs of wide structural variability. *J. Am. Chem. Soc.* 119:6072–6094
- Hong CY, Kado N, Overman LE (1993) Asymmetric synthesis of either enantiomer of opium alkaloids and morphinans. Total synthesis of (-)-and (+)-dihydrocodeinone and (-)-and (+)-morphine. *J. Am. Chem. Soc.* 115:11028–11029
- Danishefsky SJ, Masters JJ, Young WB, Link JT, Snyder LB, Magee TV, Coburn CA (1996) Total synthesis of baccatin III and taxol. *J. Am. Chem. Soc.* 118:2843–2859

34. Veisi H, Pirhayati M, Kakanejadifard A, Mohammadi P, Abdi MR, Gholami J, Hemmati S (2018) In situ green synthesis of Pd nanoparticles on tannic acid-modified magnetite nanoparticles as a green reductant and stabilizer agent: its application as a recyclable nanocatalyst (Fe<sub>3</sub>O<sub>4</sub>@ TA/Pd) for reduction of 4-nitrophenol and Suzuki reactions. *ChemistrySelect* 3:1820–1826
35. Veisi H, Tamoradi T, Karmakar B, Mohammadi P, Hemmati S (2019) In situ biogenic synthesis of Pd nanoparticles over reduced graphene oxide by using a plant extract (*Thymra spicata*) and its catalytic evaluation towards cyanation of aryl halides. *Mater. Sci. Eng. C* 104:109919–109927
36. Veisi H, Ghorbani M, Hemmati S (2019) Sonochemical in situ immobilization of Pd nanoparticles on green tea extract coated Fe<sub>3</sub>O<sub>4</sub> nanoparticles: an efficient and magnetically recyclable nanocatalyst for synthesis of biphenyl compounds under ultrasound irradiations. *Mater. Sci. Eng. C* 98:584–593
37. Tamoradi T, Veisi H, Karmakar B (2019) Pd Nanoparticle fabricated tetrahydroharman-3-carboxylic acid analog immobilized CoFe<sub>2</sub>O<sub>4</sub> catalyzed fast and expedient C–C Cross and C–S coupling. *ChemistrySelect* 4:10953–10959
38. Cyr P, Deng ST, Hawkins JM, Price KE (2013) Flow heck reactions using extremely low loadings of phosphine-free palladium acetate. *Org. Lett.* 15:4342–4345
39. Liang Y, Xie YX, Li JH (2006) Modified palladium-catalyzed Sonogashira cross-coupling reactions under copper-, amine-, and solvent-free conditions. *J. Org. Chem.* 71:379–381
40. Parker HL, Sherwood J, Hunt AJ, Clark JH (2014) Cyclic carbonates as green alternative solvents for the Heck reaction. *ACS Sustain. Chem. Eng.* 2:1739–1742
41. Hu H, Yang F, Wu Y (2013) Palladacycle-catalyzed deacetonative sonogashira coupling of aryl propargyl alcohols with aryl chlorides. *J. Org. Chem.* 78:10506–10511
42. Zhang C, Santiago CB, Crawford JM, Sigman MS (2015) Enantioselective dehydrogenative Heck arylations of trisubstituted alkenes with indoles to construct quaternary stereocenters. *J. Am. Chem. Soc.* 137:15668–15671
43. Gholinejad M, Hamed F, Biji P (2015) A novel polymer containing phosphorus–nitrogen ligands for stabilization of palladium nanoparticles: an efficient and recyclable catalyst for Suzuki and Sonogashira reactions in neat water. *Dalton Trans.* 44:14293–14303
44. Polshettiwar V, Molnár Á (2007) Silica-supported Pd catalysts for Heck coupling reactions. *Tetrahedron* 30:6949–6976
45. Yin L, Liebscher J (2007) Carbon–carbon coupling reactions catalyzed by heterogeneous palladium catalysts. *Chem. Rev.* 107:133–173
46. Mohammadinezhad A, Akhlaghinia B (2017) Fe<sub>3</sub>O<sub>4</sub>@ Boehmite-NH<sub>2</sub>-CoIINPs: an inexpensive and highly efficient heterogeneous magnetic nanocatalyst for the Suzuki-Miyaura and Heck-Mizoroki cross-coupling reactions. *Green Chem.* 19:5625–5641
47. Ghorbani-Choghamarani A, Seydyosefi Z, Tahmasbi B (2018) Zirconium oxide complex anchored on boehmite nanoparticles as highly reusable organometallic catalyst for C–S and C–O coupling reactions. *Appl. Organomet. Chem.* 32:e4396
48. Bahrami K, Kamrani SN (2018) Synthesis, characterization and application of graphene palladium porphyrin as a nanocatalyst for the coupling reactions such as: suzuki-Miyaura and Mizoroki-Heck. *Appl. Organomet. Chem.* 32:e4102
49. Babaei A, Jiang SP, Li J (2009) Electrocatalytic promotion of palladium nanoparticles on hydrogen oxidation on Ni/GDC anodes of SOFCs via spillover. *J. Electrochem. Soc.* 156:B1022–B1029
50. Putta C, Sharavath V, Sarkar S, Ghosh S (2015) Palladium nanoparticles on β-cyclodextrin functionalised graphene nanosheets: a supramolecular based heterogeneous catalyst for C–C coupling reactions under green reaction conditions. *RSC. Adv.* 5:6652–6660
51. Shaik M, Ali Z, Khan M, Kuniyil M, Assal M, Alkathlan H, Adil S (2017) Green synthesis and characterization of palladium nanoparticles using *Origanum vulgare* L extract and their catalytic activity. *Molecules* 22:165
52. Bahrami K, Targhan H (2019) A new strategy to design a graphene oxide supported palladium complex as a new heterogeneous nanocatalyst and application in carbon–carbon and carbon-heteroatom cross-coupling reactions. *Appl. Organomet. Chem.* 33:e4842
53. Meldrum FC, Heywood BR, Mann S (1992) Magnetoferritin: in vitro synthesis of a novel magnetic protein. *Science* 257(5069):522–523
54. Peng YY, Liu J, Lei X, Yin Z (2010) Room-temperature highly efficient Suzuki-Miyaura reactions in water in the presence of Stilbazol. *Green Chem.* 12:1072–1075
55. Zeng X, Zhang T, Qin Y, Wei Z, Luo M (2009) Synthesis of a carbene transfer organometallic polymer and application to forming a recyclable heterogeneous catalyst for the Suzuki reactions of aryl chlorides. *Dalton Trans.* 39:8341–8348
56. Hey DH, Orman S, Williams GH (1965) Homolytic aromatic substitution. Part XXXII. Some reactions with meta-substituted phenyl radicals. *J Chem Soc* 101–110
57. Bumagin NA, Bykov VV (1997) Ligandless palladium catalyzed reactions of arylboronic acids and sodium tetraphenylborate with aryl halides in aqueous media. *Tetrahedron* 53:14437–14450
58. Xu HJ, Zhao YQ, Zhou XF (2011) Palladium-catalyzed Heck reaction of aryl chlorides under mild conditions promoted by organic ionic bases. *J. Org. Chem.* 76:8036–8041
59. Iranpoor N, Firouzabadi H, Tarassoli A, Fereidoonzhad M (2010) 1,3,2,4-Diazadiphosphetidines as new P-N ligands for palladium-catalyzed Heck reaction in water. *Tetrahedron* 66:2415–2421
60. Cella R, Stefani HA (2006) Ultrasound-assisted synthesis of Z and E stilbenes by Suzuki cross-coupling reactions of organotellurides with potassium organotrifluoroborate salts. *Tetrahedron* 62:5656–5662
61. Veisi H, Ghorbani-Vaghei R, Hemmati S, Aliani MH, Ozturk T (2015) Green and effective route for the synthesis of monodispersed palladium nanoparticles using herbal tea extract (*Stachys lavandulifolia*) as reductant, stabilizer and capping agent, and their application as homogeneous and reusable catalyst in Suzuki coupling reactions in water. *Appl. Organomet. Chem.* 29:26–32
62. Nikoorazm M, Ghorbani-Choghamarani A, Noori N, Tahmasbi B (2016) Palladium 2-mercapto-N-propylacetamide complex anchored onto MCM-41 as efficient and reusable nanocatalyst for Suzuki, Stille and Heck reactions and amination of aryl halides. *Appl. Organomet. Chem.* 30:843–851
63. Bahrami K, Khodaei MM, Meibodi FS (2017) Suzuki and Heck cross-coupling reactions using ferromagnetic nanoparticle-supported palladium complex as an efficient and recyclable heterogeneous nanocatalyst in sodium dodecylsulfate micelles. *Appl. Organomet. Chem.* 31:e3627
64. Jabbari A, Tahmasbi B, Nikoorazm M, Ghorbani-Choghamarani A (2018) A new Pd-Schiff-base complex on boehmite nanoparticles: its application in Suzuki reaction and synthesis of tetrazoles. *Appl. Organomet. Chem.* 32:e4295
65. Faria VW, Oliveira DG, Kurz MH, Gonçalves FF, Scheeren CW, Rosa GR (2014) Palladium nanoparticles supported in a polymeric membrane: an efficient phosphine-free “green” catalyst for Suzuki-Miyaura reactions in water. *RSC. Adv.* 4:13446–13452
66. Kim S, Cho HJ, Shin DS, Lee SM (2017) Recyclable and eco-friendly Pd-complexed graphene oxide/N-heterocyclic carbene catalyst for various coupling reactions in aqueous phase. *Tetrahedron Lett.* 58:2421–2425

67. Shendage SS, Nagarkar JM (2014) Electrochemically codeposited reduced graphene oxide and palladium nanoparticles: an efficient heterogeneous catalyst for Heck coupling reaction *Colloids Interface. Sci. Commun.* 1:47–49
68. Fernández-García L, Blanco M, Blanco C, Álvarez P, Granda M, Santamaría R, Menéndez R (2016) Graphene anchored palladium complex as efficient and recyclable catalyst in the Heck cross-coupling reaction. *J. Mol. Catal. A* 416:140–146
69. Oswal P, Arora A, Kaushal J, Rao GK, Kumar S, Singh AK, Kumar A (2019) Ultra-small palladium nano-particles synthesized using bulky S/Se and N donor ligands as a stabilizer: application as catalysts for Suzuki-Miyaura coupling. *RSC. Adv.* 9:22313–22319

**Publisher's Note** Springer Nature remains neutral with regard to jurisdictional claims in published maps and institutional affiliations.